Engineering Analysis with Boundary Elements 93 (2018) 161–166

Contents lists available at ScienceDirect

Engineering Analysis with Boundary Elements

journal homepage: www.elsevier.com/locate/enganabound

A new singular element for evaluating stress intensity factors of V-shaped notches under mixed-mode load

Jianming Zhang*, Yunqiao Dong, Chuanming Ju, Weicheng Lin

State Key Laboratory of Advanced Design and Manufacturing for Vehicle Body, College of Mechanical and Vehicle Engineering, Hunan University, Changsha 410082, China

ARTICLE INFO

Keywords:
Singular element
Stress intensity factors
V-shaped notches
Boundary element method

ABSTRACT

In this paper, a new singular element is presented to evaluate stress intensity factors of V-shaped notches subjected to mixed-mode load. The proposed element takes into account special variation of displacements in the vicinity of the notch tip. The singularity at notch tip is variable unlike the crack problem where the displacements around the crack tip have variation of square root of *r*. In the proposed method, special basis functions considering the singularity order at notch tip are incorporated into the shape functions of the new element, and the singularity order is determined by the included angle of the notch. With the new element, more accurate displacement and stress fields in the neighborhood of the notch tip can be obtained, thus the stress intensity factors are computed more accurately. Accurate stress intensity factors are important for the V-notched structures to develop a fracture criterion. Numerical examples have demonstrated the accuracy and efficiency of the proposed method.

1. Introduction

Studying of V-notched structures is of great importance, since they are stress raisers. The stress at the tip of a sharp notch is singular according to the linear elastic theory. Thus the stresses evaluated at singular point have little reference value and the classical strength theories are not suitable for V-notch problems. The fracture criterion for the V-notched structures should be based on the stress intensity factors.

The boundary element method (BEM) is an attractive method for the V-notch problems due to accurate results for stresses and mesh reduction [1–15]. Rzasnicki et al. [16] applied BEM to analysis of single-edge notch subjected to pure bending. Portela et al. [17] developed a boundary element singularity subtraction technique to analyze the sharp notched plates. Niu et al. [18] proposed an interpolating matrix method coupled with conventional BEM to model singular stress field in V-notched structures. Cheng et al. [19] analyzed the singularity order of V-notch with angularly inhomogeneous elastic properties. In these methods, complicated mathematical deductions are used and they are not convenient to implement in ordinary BEM programs.

In this paper, a new singular element with special shape functions is proposed for evaluating the stress intensity factors of V-shaped notches. The element with usual shape functions cannot accurately model the displacement field around the notch tip unless extremely fine meshes are used. The singular element for crack problems is also not suitable for analyzing the structure with V-shaped notches. This is because the displacements in the vicinity of the notch tip are of the variation of r^{λ}. r is the distance to the notch tip and λ is the eigenvalue ($0.5 \le \lambda \le 1$). The crack tip singular element [20–23] can only model the variation of $r^{0.5}$.

The stress singularity is mainly determined by the first eigenvalue λ_1, especially for large included angle of the notch. In the proposed method, the variation of $r^{\lambda 1}$ is considered in the new singular element. λ_1 varies with respect to the notch angle. The special shape functions are derived according to the notch angle. With the new singular element, more accurate displacement and stress distributions in the neighborhood of the notch tip can be obtained, thus the stress intensity factor is evaluated more accurately. Accurate stress intensity factor is important for the V-notched structures to develop a fracture criterion.

This paper is organized as follows. In Section 2, the BEM is briefly described. Section 3 introduces the new singular element in detail. Numerical examples are given in Section 4. The paper ends with conclusions in Section 5.

2. Boundary element method

2.1. Boundary integral equation

The boundary integral equation for 2D elastostatic problem in an isotropic, homogeneous medium is as follows:

$$c_{ij}(P)u_j(P) = \int_{\Gamma} u^*_{ij}(P,Q)t_j(Q)d\Gamma(Q) - \int_{\Gamma} t^*_{ij}(P,Q)u_j(Q)d\Gamma(Q) \quad (1)$$

where P and Q are the source and the field points, respectively. $c_{ij}(P)$ is a coefficient matrix depending on the smoothness of the boundary Γ at the

* Corresponding author.
E-mail address: zhangjm@hnu.edu.cn (J. Zhang).

https://doi.org/10.1016/j.enganabound.2018.04.006
Received 27 February 2018; Received in revised form 24 March 2018; Accepted 12 April 2018
Available online 19 May 2018

source point P. u_j and t_j represent the displacement and traction components, respectively. $u^*_{ij}(P,Q)$ and $t^*_{ij}(P,Q)$ are the well-known Kelvin fundamental solutions and given by

$$u^*_{ij}(P,Q) = \frac{1}{8\pi G(1-\upsilon)}\left[(3-4\upsilon)\delta_{ij}\ln\frac{1}{r} + r_{,i}r_{,j}\right] \tag{2}$$

$$t^*_{ij}(P,Q) = -\frac{1}{4\pi(1-\upsilon)r}\left\{\frac{\partial r}{\partial n}\left[(1-2\upsilon)\delta_{ij} + 2r_{,i}r_{,j}\right] - (1-2\upsilon)(r_{,i}n_j - r_{,j}n_i)\right\} \tag{3}$$

where G and ν are the shear modulus and the Poisson's ratio, respectively. r is the distance between the source and the field point. n_i and n_j are the components of the normal n.

2.2. Solution of the boundary integral equation

Eq. (1) is discretized by n_e elements. The discretization form of the boundary integral equation is given by

$$c_{ij}(P)u_j(P) = \sum_{e=1}^{n_e}\left\{\sum_{\alpha=1}^{n_\alpha} t^\alpha_j \int_{\Gamma_e} u^*_{ij}(P,Q)N_\alpha(Q)d\Gamma(Q)\right\} - \sum_{e=1}^{n_e}\left\{\sum_{\alpha=1}^{n_\alpha} u^\alpha_j \int_{\Gamma_e} t^*_{ij}(P,Q)N_\alpha(Q)d\Gamma(Q)\right\} \tag{4}$$

where n_α is the number of the element nodes. N_α is the shape function of the αth node of the element.

The system of linear algebraic equations can be expressed in matrix form as

$$\mathbf{Hu} = \mathbf{Gt} \tag{5}$$

where vectors $\mathbf{u}$ and $\mathbf{t}$ consist of all nodal displacements and tractions on the boundary. Matrix $\mathbf{H}$ contains integrals involving t^*_{ij}, and matrix $\mathbf{G}$ contains integrals involving u^*_{ij}. Rearranging Eq. (5) according to the boundary conditions, the final system of linear equations can be obtained.

$$\mathbf{Ax} = \mathbf{f} \tag{6}$$

where $\mathbf{A}$ is the coefficient matrix. $\mathbf{x}$ is the vector containing the boundary unknowns at the source nodes. $\mathbf{f}$ is the known vector on the right-hand side.

3. New singular element

3.1. Analysis of the singularity for the V-shaped notch

The asymptotic stress fields around the notch tip are given by [24]

$$\sigma_r = \frac{S_{\mathrm{I}}}{\sqrt{2\pi}(r)^{1-\lambda_1}}\left\{-\cos(1+\lambda_1)\theta - \frac{(3-\lambda_1)\sin(1+\lambda_1)\alpha}{(1-\lambda_1)\sin(1-\lambda_1)\alpha}\cos(1-\lambda_1)\theta\right\} + \frac{S_{\mathrm{II}}}{\sqrt{2\pi}(r)^{1-\lambda_2}}\left\{\sin(1+\lambda_2)\theta + \frac{(3-\lambda_2)\sin(1+\lambda_2)\alpha}{(1+\lambda_2)\sin(1-\lambda_2)\alpha}\sin(1-\lambda_2)\theta\right\} \tag{7}$$

$$\sigma_\theta = \frac{S_{\mathrm{I}}}{\sqrt{2\pi}(r)^{1-\lambda_1}}\left\{\cos(1+\lambda_1)\theta - \frac{(1+\lambda_1)\sin(1+\lambda_1)\alpha}{(1-\lambda_1)\sin(1-\lambda_1)\alpha}\cos(1-\lambda_1)\theta\right\} + \frac{S_{\mathrm{II}}}{\sqrt{2\pi}(r)^{1-\lambda_2}}\left\{\sin(1+\lambda_2)\theta - \frac{\sin(1+\lambda_2)\alpha}{\sin(1-\lambda_2)\alpha}\cos(1-\lambda_2)\theta\right\} \tag{8}$$

$$\sigma_{r\theta} = \frac{S_{\mathrm{I}}}{\sqrt{2\pi}(r)^{1-\lambda_1}}\left\{\sin(1+\lambda_1)\theta - \frac{\sin(1+\lambda_1)\alpha}{\sin(1-\lambda_1)\alpha}\sin(1-\lambda_1)\theta\right\} + \frac{S_{\mathrm{II}}}{\sqrt{2\pi}(r)^{1-\lambda_2}}\left\{\cos(1+\lambda_2)\theta - \frac{(1-\lambda_2)\sin(1+\lambda_2)\alpha}{(1+\lambda_2)\sin(1-\lambda_2)\alpha}\cos(1-\lambda_2)\theta\right\} \tag{9}$$

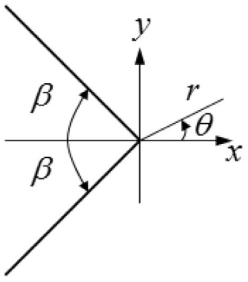

Fig. 1. V-shaped notch.

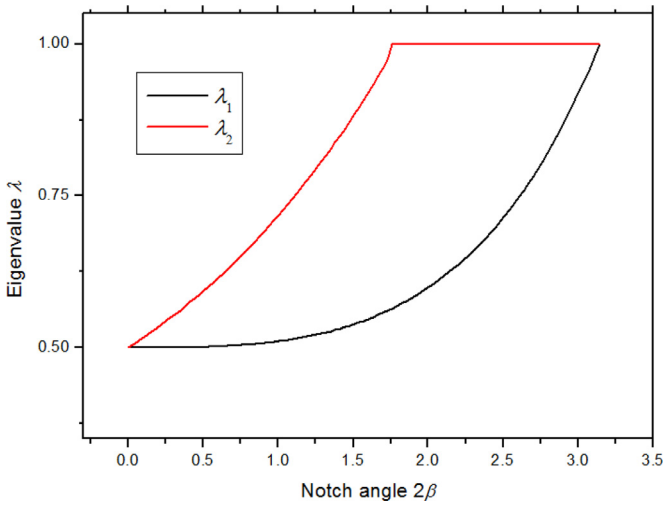

Fig. 2. Variations of λ_1 and λ_2 with respect to the notch angle 2β.

The asymptotic displacement fields are as follows [24]:

$$u_r = \frac{S_I(r)^{\lambda_1}}{\sqrt{2\pi}G}\left\{-\frac{1}{2\lambda_1}\cos(1+\lambda_1)\theta + \frac{\sin(1+\lambda_1)\alpha}{(1-\lambda_1)(1-t)\sin(1-\lambda_1)\alpha}\cos(1-\lambda_1)\theta\right\} + \frac{S_{II}(r)^{\lambda_2}}{\sqrt{2\pi}G}\left\{-\frac{1}{2\lambda_2}\sin(1+\lambda_2)\theta + \frac{\sin(1+\lambda_2)\alpha}{(1+\lambda_2)(1-t)\sin(1-\lambda_2)\alpha}\sin(1-\lambda_2)\theta\right\} \tag{10}$$

$$u_\theta = \frac{S_{\mathrm{I}}(r)^{\lambda_1}}{\sqrt{2\pi}G}\left\{\frac{1}{2\lambda_1}\sin(1+\lambda_1)\theta - \frac{t\sin(1+\lambda_1)\alpha}{(1-\lambda_1)(1-t)\sin(1-\lambda_1)\alpha}\sin(1-\lambda_1)\theta\right\} + \frac{S_{\mathrm{II}}(r)^{\lambda_2}}{\sqrt{2\pi}G}\left\{-\frac{1}{2\lambda_2}\cos(1+\lambda_2)\theta + \frac{t\sin(1+\lambda_2)\alpha}{(1+\lambda_2)(1-t)\sin(1-\lambda_2)\alpha}\cos(1-\lambda_2)\theta\right\} \tag{11}$$

where r, θ denotes a polar co-ordinate system centered at the notch tip as shown in Fig. 1; S_{I}, S_{II} and t are constants; G is the shear modulus; the included angle of the notch is 2β and $\alpha = \pi - \beta$; eigenvalues λ_1 and λ_2 are determined by following characteristic equations:

$$\lambda_1\sin(2\alpha) + \sin(2\lambda_1\alpha) = 0 \tag{12}$$

$$\lambda_2\sin(2\alpha) - \sin(2\lambda_2\alpha) = 0 \tag{13}$$

The stress intensity factors are defined as follows:

$$K_{\mathrm{I}} = \lim_{r\to 0}\sqrt{2\pi}(r)^{1-\lambda_1}\sigma_\theta\big|_{\theta=0} \tag{14}$$

$$K_{\mathrm{II}} = \lim_{r\to 0}\sqrt{2\pi}(r)^{1-\lambda_2}\sigma_{r\theta}\big|_{\theta=0} \tag{15}$$

λ_1 and λ_2 vary with respect to the notch angle as shown in Fig. 2. From this figure, we can see that the stress singularity is mainly determined by λ_1, especially for large notch angle. This feature provides convenience for us to get the special shape functions of the new element.

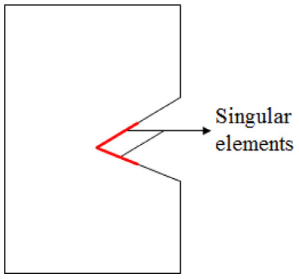

Fig. 3. Positions of the singular element.

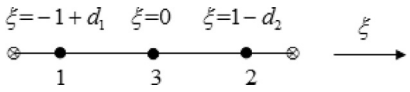

Fig. 4. Singular quadratic element.

3.2. Special shape functions of the new singular element

In section 3.1, we have analyzed the singularity of the stress. The stress and displacement fields are mainly dependent on λ_1. Therefore, the variation of $r^{\lambda 1}$ is considered in the new singular element to model the special displacement field around the notch tip. The new singular elements are collocated around the notch tip as shown in Fig. 4. (Fig. 3).

The deduction of the special shape functions for the new singular element is introduced in this part. We assume that the node ($\xi=-1$) of the singular quadratic element shown in Fig. 4 lies on notch tip. The distance r is proportional to $(1+\xi)$. In order to get the variation of $r^{\lambda 1}$, the special shape function should be following form:

$$N^i = a_0^i + a_1^i(1+\xi)^{\lambda_1} + a_2^i(1+\xi)^{2\lambda_1} + a_3^i(1+\xi)^{3\lambda_1} \tag{15}$$

where $i=0,\ldots,3$; N^i denotes the shape function of the ith node; $a_0^i \sim a_3^i$ are unknown coefficients to be solved.

The shape functions in Eq. (15) must satisfy the conditions:

$$N^i(\xi_j) = \delta_{ij} \tag{16}$$

where $i, j=0,\ldots,3$; δ_{ij} is Kronecker delta function; ξ_j are the local node coordinates of the new element as shown in Fig. 4.

Using Eq. (16) for each i in Eq. (15), a set of 4×4 linear system of equations is obtained. Solving this system of equations will yield the coefficients $a_0^i \sim a_3^i$.

The special shape functions of other singular elements (linear, cubic or higher order singular elements) can be obtained by the similar method. The offsets d_1 and d_2 shown in Fig. 4 can be zero or non-zero, thus the special shape functions of continuous, discontinuous and semi-discontinuous singular elements are derived in a uniform method.

4. Numerical examples

4.1. An inclined V-notched plate under uniaxial tension load

An inclined V-notched plate under uniaxial tension load σ is concerned in this example. The bisector of the notch, included angle $2\beta=\pi/6$, makes an angle $\alpha=\pi/4$ with the x global axis. Plane strain case with Young's modulus $E=1$ (in consistent units), Poisson's ratio $\nu=0.25$, $h/w=2$ and $a/w=0.5$ are considered as shown in Fig. 5.

Fig. 6 shows the displacements U_y along edge e around the notch tip. 'Reference solution' denotes the result by the FEM with 3,641,007 nodes. 'Singular quadratic element' and 'Singular cubic element' represent the results by the BEM with the proposed singular elements. 'Traditional quadratic element' and 'Traditional cubic element' mean the results by the BEM with traditional elements. Quadratic element with 287 nodes and cubic element with 280 nodes are used in the BEM, respectively.

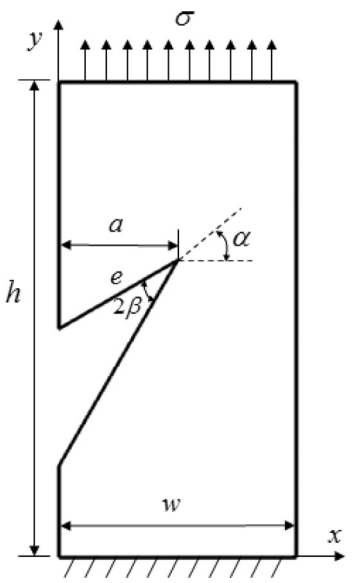

Fig. 5. An inclined V-notched plate under uniaxial tension load.

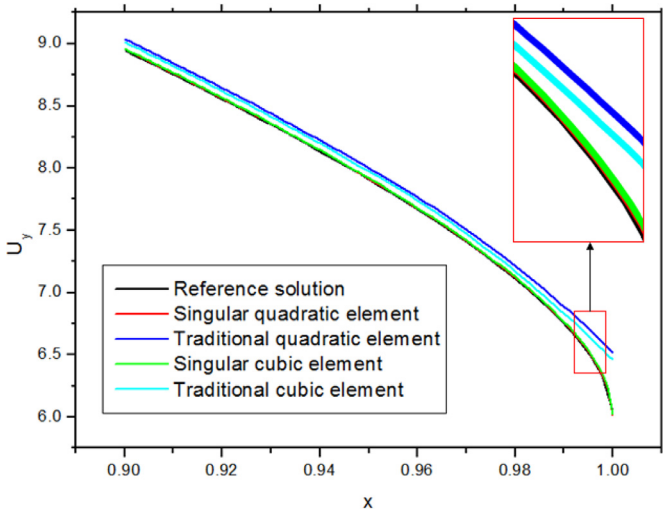

Fig. 6. Displacements along edge e obtained by different methods.

From Fig. 6, one can see that with the new element, more accurate displacement distributions around the notch tip can be obtained.

The normalized stress intensity factors $K_I/\sigma\sqrt{\pi a}$ and $K_{II}/\sigma\sqrt{\pi a}$ by different methods with a series of nodes are shown in Figs. 7 and 8, respectively. It can be seen that the stress intensity factors K_I and K_{II} are convergent as the number of mesh nodes increases. Except singular quadratic element for K_{II}, the results obtained by the proposed method are closer to the convergence value, especially when fewer nodes are used.

4.2. Plate with a square hole under uniaxial tension load

In this example, the plate containing a square hole under uniaxial tension load σ is in plane strain state with Young's modulus $E=1$ (in consistent units), Poisson's ratio $\nu=0.25$, $w=4$, $h=4$, $a=2$ and $d=1$ as shown in Fig. 9.

Fig. 10 shows the displacements U_y along edge e around the notch tip. 'Reference solution' denotes the result by the FEM with 4,004,000 nodes. 'Singular quadratic element' and 'Singular cubic element' represent the results by the BEM with the proposed singular elements. 'Tra-

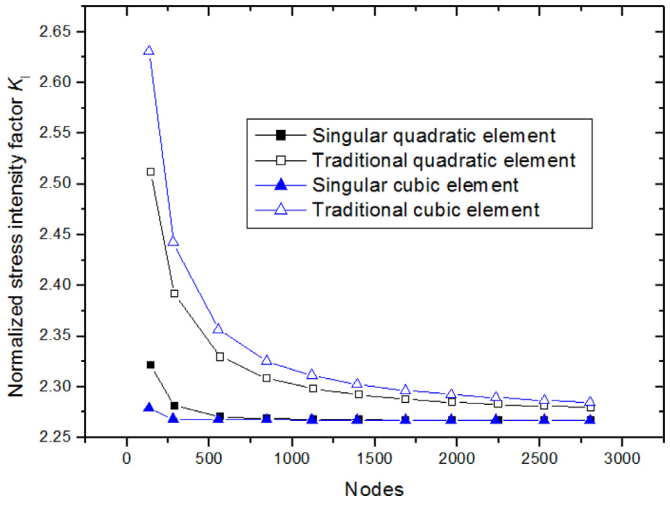

Fig. 7. Normalized stress intensity factor $K_I/\sigma\sqrt{\pi a}$.

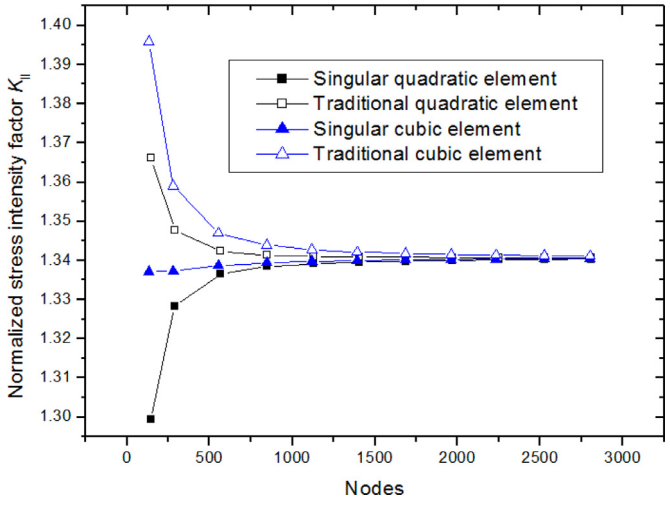

Fig. 8. Normalized stress intensity factor $K_{II}/\sigma\sqrt{\pi a}$.

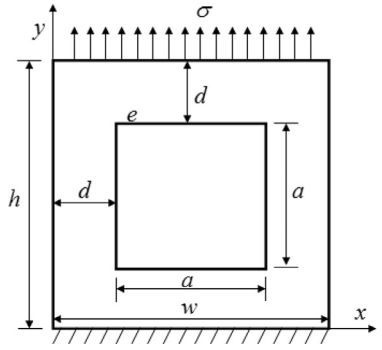

Fig. 9. Plate with a square hole under uniaxial tension load.

ditional quadratic element' and 'Traditional cubic element' mean the results by the BEM with traditional elements. 168 and 152 nodes are used in the BEM with quadratic and cubic element, respectively. From Fig. 10, we can see that with the new element, more accurate displacement distributions around the notch tip can be obtained.

The normalized stress intensity factors $K_I/\sigma\sqrt{\pi a}$ and $K_{II}/\sigma\sqrt{\pi a}$ by different methods with a series of nodes are shown in Figs. 11 and 12, respectively. From these two figures it can be found that the stress intensity factors K_I and K_{II} are convergent as the number of mesh nodes

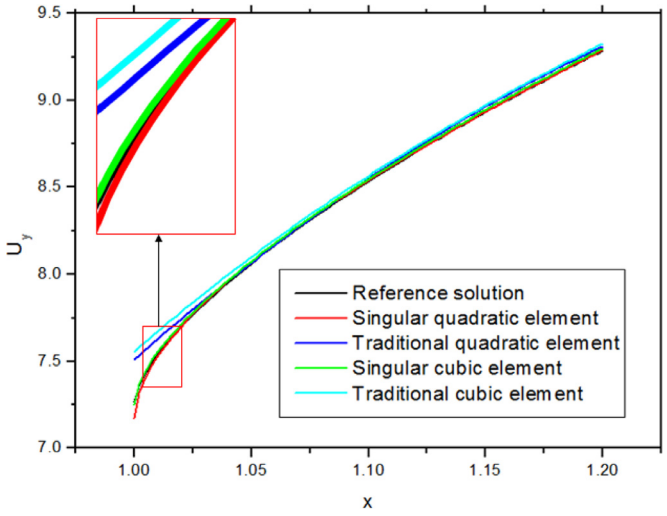

Fig. 10. Displacements along edge e obtained by different methods.

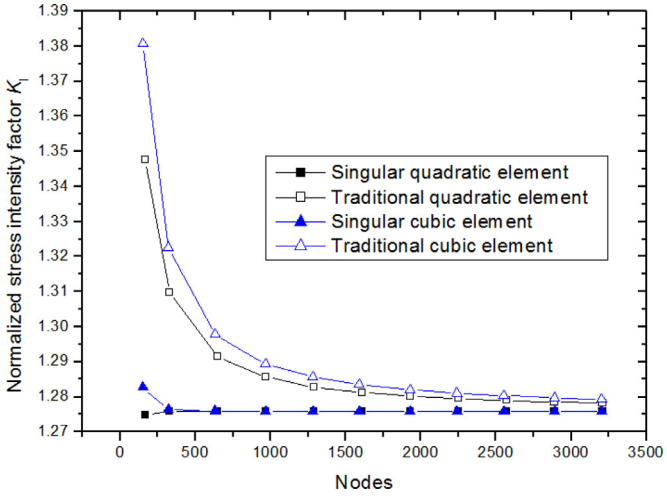

Fig. 11. Normalized stress intensity factor $K_I/\sigma\sqrt{\pi a}$.

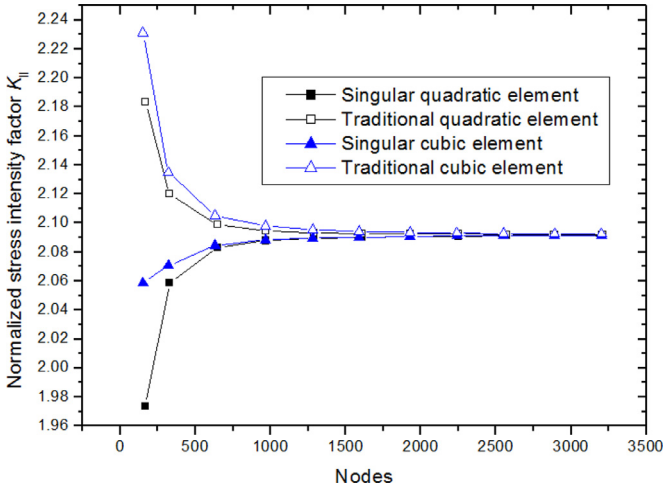

Fig. 12. Normalized stress intensity factor $K_{II}/\sigma\sqrt{\pi a}$.

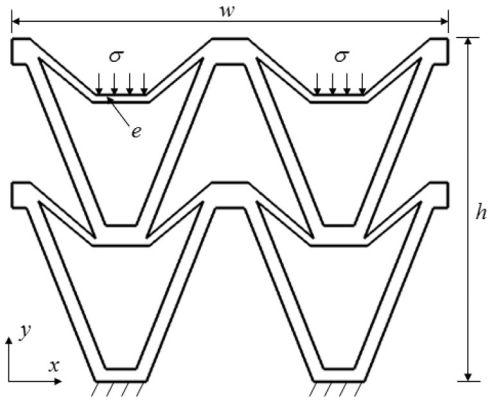

Fig. 13. Thin-wall structure with many V-notches.

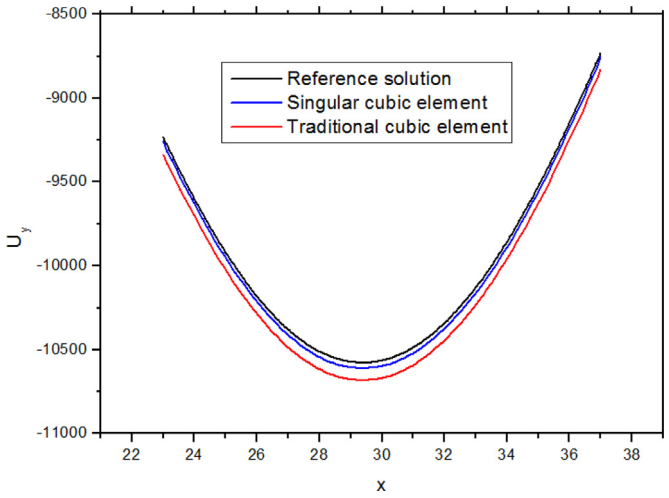

Fig. 14. Displacements along edge *e* obtained by different methods.

increases. Except singular quadratic element for K_{II}, the results obtained by the proposed method are closer to the convergence value, especially when fewer nodes are used.

4.3. Thin-wall structure with many V-notches

In the last example, a thin-wall structure with many V-notches is considered as shown in Fig. 13. Plane strain case with Young's modulus $E=1$ (in consistent units), Poisson's ratio $\nu=0.25$, uniaxial tension load $\sigma=1$, $w=120$ and $h=95$ are assumed.

Fig. 14 shows the displacements U_y along edge *e*. 'Reference solution' denotes the result by the FEM with 3,958,580 nodes. 'Singular cubic element' represents the results by the BEM with the proposed singular cubic element. 'Traditional cubic element' means the results by the BEM with traditional cubic element. 3030 nodes are used in these two methods. From Fig. 14, we can see that with the new element, more accurate displacement distributions around the notch tip can be obtained. The von Mises stress by the proposed method is shown in Fig. 15. This illustrates that the proposed method is able to solve the V-notch problem with complicated structure.

5. Conclusion

A new singular element is proposed to evaluate stress intensity factors of V-shaped notches subjected to mixed-mode load in this paper. The displacements in the vicinity of the notch tip have the variation of r^{λ}. The traditional elements with usual shape functions do not lead to accurate solutions unless extremely fine meshes are used. In the proposed method, special basis functions considering the stress singularity at notch tip are incorporated into the shape functions of the new element. Numerical results have demonstrated that compared with traditional element, the displacements obtained by our method around the notch tip is more accurate and higher level of accuracy for stress intensity factors can be obtained. Accurate stress intensity factors are important for the V-notched structures to develop a fracture criterion.

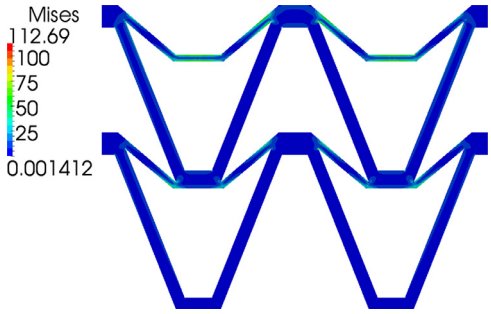

Fig. 15. Von Mises stress by the proposed method with 3030 nodes.

Acknowledgment

This work was supported in part by National Science Foundation of China under grant numbers 11772125 and 11472102.

References

[1] Brebbia CA, Telles JCF, Wrobel LC. Boundary element techniques: theory and applications in engineering, 5. Berlin: Springer-Verlag; 1984.
[2] Cheng AHD, Cheng DT. Heritage and early history of the boundary element method. Eng Anal Boundary Elem 2005;29:268–302.
[3] Zhang JM, Zhong YD, Dong YQ, et al. Expanding element interpolation method for analysis of thin-walled structures. Eng Anal Boundary Elem 2018;86:82–8.
[4] Zhang JM, Lin WC, Dong YQ, et al. A double-layer interpolation method for implementation of BEM analysis of problems in potential theory. Appl Math Modell 2017;51:250–69.
[5] Yao ZH. A new type of high-accuracy BEM and local stress analysis of real beam, plate and shell structures. Eng Anal Boundary Elem 2016;65:1–17.
[6] Zhang JM, Huang C, Lu CJ, et al. Automatic thermal analysis of gravity dams with fast boundary face method. Eng Anal Boundary Elem 2014;41:111–21.
[7] Zhou FL, Li Y, Zhang JM, et al. A time step amplification method in boundary face method for transient heat conduction. Int J Heat Mass Transfer 2015;84:671–9.
[8] Dong YQ, Zhang JM, Xie GZ, et al. A general algorithm for the numerical evaluation of domain integrals in 3D boundary element method for transient heat conduction. Eng Anal Boundary Elem 2015;51:30–6.
[9] Zhang JM, Qin XY, Han X, et al. A boundary face method for potential problems in three dimensions. Int J Numer Methods Eng 2009;80(3):320–37.
[10] Liu YJ, Fan H. Analysis of the thin piezoelectric solids by the boundary element method. Comput Methods Appl Mech Eng 2002;191:2297–315.
[11] Ma H, Kamiya N. A general algorithm for the numerical evaluation of nearly singular boundary integrals of various orders for two- and three-dimensional elasticity. Comput Mech 2002;29(4):277–88.
[12] Gao XW, Zhang JB, Zheng BJ, et al. Element-subdivision method for evaluation of singular integrals over narrow strip boundary elements of thin-walled and slender structures. Eng Anal Boundary Elem 2016;66:145–54.
[13] Zhao P, Qin TY, Zhang LN. A regularized time-domain BIEM for transient elastodynamic crack analysis in piezoelectric solids. Eng Anal Boundary Elem 2015;56:145–53.
[14] Dong CY, Xie ZC, Yao ZH, et al. Some numerical solution methods of hypersingular integrals in BIE. Adv Mech 1995;25(3):424–9.
[15] Sladek V, Sladek J, Tanaka M. Nonsingular BEM formulations for thin-walled structures and elastostatic crack problems. Acta Mech 1993;99(1–4):173–90.
[16] Rzasnicki W, Mendelson A. Application of boundary integral method to elastoplastic analysis of V-notched beams. Int J Fracture 1975;11(2):329–42.
[17] Portela A, Aliabadi MH, Rooke DP. Efficient boundary element analysis of sharp notched plates. Int J Numer Methods Eng 1991;32(3):445–70.
[18] Niu ZR, Cheng CZ, Ye JQ, et al. A new boundary element approach of modeling singular stress fields of plane V-notch problems. Int J Solids Struct 2009;46(16):2999–3008.
[19] Cheng CZ, Ge SY, Yao SL, et al. Singularity analysis for a V-notch with angularly inhomogeneous elastic properties. Int J Solids Struct 2016;78:138–48.
[20] Xie GZ, Zhang JM, Huang C, et al. A direct traction boundary integral equation method for three-dimension crack problems in infinite and finite domains. Comput Mech 2014;53(4):575–86.

[21] Xie GZ, Zhang DH, Meng FN, et al. Calculation of stress intensity factor along the 3D crack front by dual BIE with new crack front elements. Acta Mech 2017;228(9):3135–53.
[22] Ariza MP, Saez A, Dominguez J. A singular element for three-dimensional fracture mechanics analysis. Eng Anal Boundary Elem 1997;20(4):275–85.
[23] Mi Y, Aliabadi MH. Discontinuous crack-tip elements: application to 3D boundary element method. Int J Fracture 1994;67(3):R67–71.
[24] Kuang ZB, Ma FS. Crack tip fields (in Chinese). Xi'an: Xi'an Jiaotong University Press; 2002.